Available online at www.sciencedirect.com
ScienceDirect
Carbohydrate Polymers 73 (2008) 231–240
Carbohydrate Polymers
www.elsevier.com/locate/carbpol

Development of a precipitation method intended for the entrapment of hydrated salt

Fabien Salaün [a,*], Eric Devaux [a], Serge Bourbigot [b], Pascal Rumeau [c]

[a] GEMTEX-ENSAIT, 9 rue de l'ermitage, BP 30329, 59100 Roubaix, France
[b] Procédés d'Élaboration des Revêtements Fonctionnels (PERF), LSPES UMR-CNRS 8008, École Nationale Supérieure de Chimie de Lille (ENSCL), BP 90108, 59652 Villeneuve d'Ascq Cedex, France
[c] IFTH, 2 rue de la recherche, 59656 Villeneuve D'ASCQ, France

Received 23 July 2007; received in revised form 24 October 2007; accepted 14 November 2007
Available online 22 November 2007

Abstract

Microcapsules loaded by sodium phosphate dodecahydrate (DSP) were prepared according to the solvent evaporation–precipitation method using chloroform as solvent and cellulose acetate butyrate (CAB) cross-linked by methylene diisocyanate (MDI) as coating polymer. The effects of the preparation conditions on the capsule morphology and the entrapment efficiency of water-soluble materials were investigated. A mechanism of the process of wall formation material is also suggested depending on the ratio of CAB/MDI introduced. A competition between the hydroxyl functions of CAB and water to react with an isocyanate might occur to form the microcapsule shell. An increase of the amount of MDI promoted urethane linkages whereas urea and urethane linkages decreased by increasing the CAB amount. Furthermore, the encapsulation yield was found to be linked to the CAB and MDI concentrations and optimal when the ratio (MDI to CAB) was in the range of 0.4–1.

Keywords: Microcapsules; Methylene diisocyanate; Cellulose acetate butyrate; Interfacial precipitation; Interfacial polymerization

1. Introduction

Preparation of uniform polymeric microcapsules in the 1–10 μm size range has received great attention in recent years and more especially for their use in textile area (Erkan & Sariisik, 2004; Nelson, 1991, 2002). Amongst these applications, the incorporation of microencapsulated phase change materials (PCMs) has attracted great interest to improve thermal insulation (Leitch & Tassinari, 2000; Pause, 1995). Until now, only organic PCMs have been encapsulated (Hawlader, Uddin, & Khin, 2003; Yoshizawa, Kamio, Hirabayashi, Jacobson, & Kitamura, 2004; Zhang, Tao, Yick, & Wang, 2004). It has been found that the possible use of salt hydrates and their supercooling property can be exploited for specialized thermal storage applications (Hirano & Saitoh, 2002; Hirano, Saitoh, Oya, & Yamazaki, 2001; Sandnes & Rekstad, 2006). Furthermore, a step of encapsulation with a semi-impermeable coating is necessary to improve their performance since hydrated salts are sensible to moisture (Canbazoğlu, Şahinaslan, Ekmekyapar, Aksoy, & Akarsu, 2005).

The functional performance of the microcapsules depends on the morphology, the chemical nature and the surface characteristics of the polymeric shell influenced by the process parameters (Yadav, Suresh, & Khilar, 1990). The choice of a particular process is determined by the solubility characteristics of the active compound and the shell material. Cellulose derivatives have been widely used in the preparation of water-soluble microencapsulated compound. Microencapsulation processes using cellulose acetate butyrate (CAB) as coating material include emulsion solvent evaporation (Arnaud, Boue, & Chaumeil, 1996; El Bahri & Taverdet, 2006; Obeidat & Price, 2005;

* Corresponding author. Tel.: +33 3 20 25 64 59; fax: +33 3 20 27 25 97.
E-mail address: fabien.salaun@ensait.fr (F. Salaün).

0144-8617/$ - see front matter © 2007 Elsevier Ltd. All rights reserved.
doi:10.1016/j.carbpol.2007.11.020

Torres, Boado, Blanco, & Vila-Jato, 1998), spray drying (Giunchedi, Conti, Maggi, & Conte, 1994), and precipitation (Rege et al., 1999).

In a solvent evaporation technique, morphology of CAB microcapsules is affected by the solvent choice and its evaporation temperature. Indeed, a high temperature allows a rapid shell formation characterized by a homogeneous and porous structure with large pores, while at low temperature a more compacted heterogeneous porous structure is obtained (Fundueanu et al., 2005). Besides, the pressure created by the swelling of the core component is sufficient to cause rupture of the CAB shell.

The thermo-chemical and physical properties of the CAB polymeric film can be improved by cross-linking CAB with a diisocyanate (Uda & Hijikigawa, 1988). The cellulosic compound is cross-linked through the formation of urethane bonds. Laskar, Vidal, Fichet, Gauthier, and Teyssié (2004) have observed that the required molar ratio of cross-linker (diisocyanate) to free OH groups in cellulose to obtain a network decreased with the increase of CAB amount. This result suggests two ways of cross-linking amongst the amount of CAB, inter or intra chains.

In a water in oil polycondensation system to prepare polyurethane network, it is known that the reaction of isocyanate groups with water molecules during the capsule formation forms also urea cross-linkings. This formation depends on the water molecules diffusion through the polyurethane network and could influence the thermal properties controlling the permeation properties of the microcapsules. In this work, the synthesis and characterization of poly(urea–urethane) microcapsules are studied using different amount of cellulose acetate butyrate and diphenyl methylene diisocyanate (MDI). The experimental procedure is derived from an interfacial polycondensation used for the polyurethane microcapsule preparation. The objective of this work was to investigate the influence of incorporated CAB and MDI amounts on chemical structure of microcapsules by Fourier-transform infrared spectroscopy (FTIR) analysis.

2. Experimental

2.1. Materials

Cellulose acetate butyrate (CAB) (13.5%-wt acetyl and 38%-wt butyryl content, average Mn ca. 30,000) and diphenyl methylene diisocyanate (MDI) (Suprasec 2030, Hüntsman ICI; blend of MDI isomers, 4,4′-diphenyl methylene diisocyanate principally) used as shell-forming monomers were obtained from Aldrich and Huntsman ICI. Sodium phosphate dodecahydrate, Na_2HPO_4, $12H_2O$ (DSP) was employed as core material. Nonionic surfactant, Span® 85 (sorbitan trioleate) and poly(ethylene glycol)dioleate (PEG 400 dioleate) were purchased from Aldrich, and used as emulsifier. Toluene and chloroform were of reagent grade and used without further purification.

2.2. Preparation of microcapsules

The preparation of the microcapsules was carried out according to the following method. 12.5 ml of an aqueous phase containing 15 g of hydrated salt were emulsified at a stirring rate of 8500 rpm with a homogenizer (ultra turrax®, Ika, Germany) at room temperature in 50 ml of an organic phase. The organic phase was prepared by dissolving the surfactant in a nonvolatile solvent, e.g. toluene. After 15 min, when the expected droplet size of the emulsion was reached, a solution containing 0, 0.625, 1.25, 2.5, 5 and 10%-wt of CAB previously solubilized in 30 ml of a volatile solvent (chloroform) is added. The mixture was stirred continuously using a blade stirrer at a lower speed (600 rpm) under ambient pressure and the temperature was increased at 1 °C/min until 60 °C to allow the progressive evaporation of volatile solvent. The complete cross-linking of the microcapsules was carried on by a drop-wise addition of a solution containing 0.5, 1, 2, 5, and 10%-wt of MDI in toluene, until the polycondensation was complete (2 h). The resultant microcapsules were recovered by filtration and washed with toluene to remove remaining MDI and dried at room temperature for one night.

The encapsulation yield was calculated as the ratio of the mass of microcapsules shell [after correction of salt content determined by thermogravimetric analysis (TGA) (Table 2)] obtained at the end of the process and the mass of initial substances added including CAB and MDI.

2.3. Analysis of the microcapsules

The structure of the shell polymer was analyzed by FT-IR spectra. Samples were ground and mixed with KBr to make pellets. FT-IR spectra in the transmission mode were recorded using a Nicolet Nexus, connected to a PC, in which the number of scan was 32 and the resolution was 4 cm^{-1}.

To put an interpretation on a more quantitative basis, we performed the de-convolution of the spectra using peakfit 4.0 software (Jandel, San Rafael, CA) in the 1575–1800 cm^{-1} region into Gaussian peaks. These wavenumbers were used as initial parameters for curve fitting with Gaussian component peaks. Position, bandwidths, and amplitudes of the peaks were varied until: (i) the resulting bands shifted by no more than 4 cm^{-1} from the initial parameters, (ii) all the peaks had reasonable half-widths ($<$20–25 cm^{-1}) and (iii) good agreement between the calculated sum of all components and the experimental spectra was achieved ($r^2 > .99$). The results of four independent experiments were averaged.

The relative contents of different absorption bands of elements were estimated by dividing the areas of individual peaks, assigned to particular secondary structure, by the whole area of the resulting ester band.

The thermal behavior of the particles was recorded using a TA instrument type DSC 2920 piloted on PC with

TA Advantage control software. Indium was used as standard for temperature calibration and the analysis was made under a constant stream of nitrogen (50 ml/min). Samples were placed in aluminum pans which were hermetically sealed before being placed on the calorimeter thermocouples. The sample space was purged with nitrogen at a constant flow (50 ml/min) during the experiments. Glass temperatures were obtained from at least four independent experiments on (4.0) – mg samples with a scanning speed of 20 K min^{-1}.

Thermogravimetric analyser (TA Instruments type TGA 2950) was used to record the thermograms in the temperature range from 30 to 1000 °C with a heating rate of 10 K min^{-1} in a flow of nitrogen gas at 60 ml min^{-1}. Previous thermogravimetric study (Ghule, Bhonghale, & Chang, 2003) reporting the thermal dehydration and condensation processes of disodium hydrogen dodecahydrate show a loss of 59.3% weight in the entire dehydration process contributing to the loss of 12 water molecules between 30 and 84 °C. Furthermore, in the temperature range from 246 to 345 °C, Na_4PO_7 formation resulting to the condensation process was observed. Between 345 and 600 °C no weight loss was observed. Besides, the thermal degradation of CAB/MDI occurs between 200 and 550 °C. Thus, the salt content was calculated as the ratio of the residual weight at 600 °C divided by the residual weight at 200 °C corresponding to the weight of the fully dehydrated salt and the microcapsules containing the fully dehydrated salt, respectively.

The microscopic aspects of the microcapsules were analyzed by scanning electron microscopy (SEM) (Philips XL30 ESEM/EDAX-SAPPHIRE). Energy-dispersive X-ray spectroscopy observation was performed on an EDAX instrument to observe the presence of salt in the particles. The results obtained with EDAX analyses were brought back to the same scale to allow the comparison of the various samples, by assuming that all the salt introduced is encapsulated at the end of the synthesis. Thus, the presence of elements like carbon and oxygen can be attributable to the reagents introduced for the membrane formation.

3. Results and discussion

3.1. Mechanism of formation

The polymeric capsules can be prepared from either monomers as starting materials or from oligomers and preformed polymers (Arshady, 1989). The process involves an aqueous dispersed phase in an oil continuous phase to induce the precipitation of the polymeric materials at the droplet interface. The dispersed phase is a good solvent for the monomers but acts as a non-solvent for the produced polymer (Arshady & George, 1993). Therefore during polymerization, the system is composed of three mutually immiscible phases (Wang, Fu, & Yu, 1994). When multifunctional monomers are used, a three-dimensional cross-linked system is obtained. For polyurethane or polyurea networks prepared from isocyanate and diols, the reaction of isocyanate groups with water molecules was promoted during the shell formation process that also forms urea cross-link (Lyman, 1972). The type and the amount of isocyanate and the content of water in the dispersed phase can modify the release behavior, the morphologies and the loading content of the microcapsules (Hong & Park, 1999; Lukaszczyk & Urbas, 1997).

According to the process described above, it is clear that all properties of the membrane depend not only on its chemical nature but also on all the experimental conditions of the preparation. In order to control the morphology and to prepare the microcapsules having the desired physical properties, the knowledge of the shell formation is necessary. Microencapsulation of hydrated salt was carried out by interfacial polycondensation of isocyanate with cellulose acetate butyrate and/or water. To obtain a better understanding of the particle formation we have studied the influence of the CAB–MDI ratio on the microcapsule morphology and on the formed shell chemistry.

3.1.1. Emulsification step

First, a stable inverse emulsion is formed by controlling the shearing of an aqueous solution containing hydrated salt in toluene. This step may be influenced by physical parameters such as the mixer and the vessel configuration, the speed of mixing and the volume ratio of the two phases, and also by physicochemical properties such as the interfacial tension, the respective viscosities, the densities and the chemical composition of the two phases in contact. Preliminary experiments were carried out to optimize the formation of a stable inverse emulsion according to the required hydrophilic–lipophilic balance (HLB) concept of Griffin (1949). The surfactants used were mixtures of Span® 85 and PEG 400 dioleate in different proportions in order to result in HLB values covering the range 1.8–8. Emulsions, consisting of hydrated salt, toluene and Span® 85 and/or PEG 400 dioleate as surfactant, were prepared under high shear (8500 rpm) to estimate the emulsion stability. Emulsion stability was judged by the appearance and by observing phase separation, if any, by bare eye observation and under microscope 4 h after preparation. Table 1 shows the different surfactant systems

Table 1
Influence of the HLB values of a Span® 85/dioleate PEG 400 mixture on the emulsion type, stability and particle size distribution

HLB of surfactants Span® 85/dioleate PEG 400	Type	Emulsion stability*	Particle size distribution
1.8	w/o	+++	Very narrow
2	w/o	+++	Very narrow
3	w/o	++	Narrow
4	w/o	+ (Coalescence)	Narrow
5	w/o	+ (Coalescence)	Bimodal
6	w/o	– (Coalescence)	Bimodal
7	w/o	– (Sedimentation)	Broad
8	o/w/o	– (Sedimentation)	Very broad

* Classification: +++, excellent; ++, good; +, satisfactory; –, poor.

tested for emulsification. The emulsions obtained using a low HLB were found to be stable. And, it had been observed under microscope that the average droplet size for the emulsion prepared using Span® 85 ranged between 0.5 and 2 μm.

3.1.2. Formation of the cross-linked microparticles

In this paper, in order to limit the number of parameters and to facilitate the analysis, this step was optimized to obtain a mean particle diameter above 1 μm with a fixed amount of surfactant (2.5%-wt of Span® 85) and a shearing rate of 8500 rpm. Once the desirable mean diameter is obtained, the stirring is reduced to 600 rpm and a solution of CAB in chloroform is added. Quite rapidly the CAB polymer film precipitates at the organic side of the interface and the reaction slows down since the diffusion of water becomes restricted by the polymeric wall. The thickness of the wall increases slowly and the growth occurs on the organic side with the adding of MDI in the last step. During this growth, the layer morphology changes and it becomes less porous.

The reaction of the shell formation is given in Schemes 1 and 2. The polyurethane shell is formed by reaction of the hydroxyl groups of CAB with isocyanate groups of MDI at the interface (Scheme 2). Interfacial polymerization occurs rapidly at 60 °C. Furthermore, MDI monomers can be hydrolyzed slowly at the interface to form amines which react with MDI monomer to form a part of the shell (Scheme 1) (Lukaszczyk & Urbas, 1997). This latter reaction occurs on the oil side of the interface and depends on the water molecules diffusion through the CAB–MDI network. The polymeric shell was formed and grown in the organic phase, illustrated by the fact that both isocyanate and the derived amine entities formed are both liposoluble. Thus, the nature of the component and the composition of this phase should affect the course of polycondensation reaction.

Close examination of electron micrographs of some of the products, of those exhibiting 0.625% and 1.25% of CAB (Fig. 1), shows that the microcapsules are mass coagulates of much smaller microcapsules. The particles seem all the more aggregate as the rates of CAB and MDI increase. Nevertheless, the mean average diameter is higher than 1 μm. Another parameter to be taken into an account to interpret the results of the change of morphology is the variation of the viscosity of the media containing isocyanate and the swellability of the polymer. This parameter

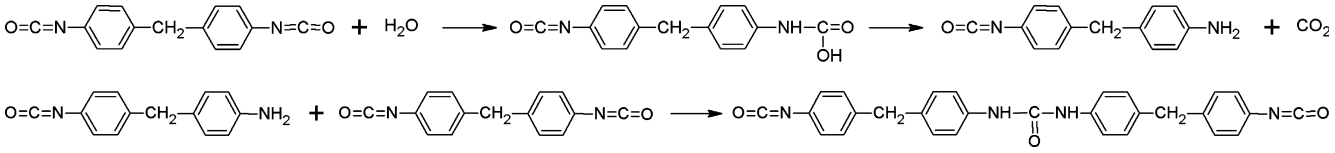

Scheme 1. Wall forming reaction of polyurea microcapsule.

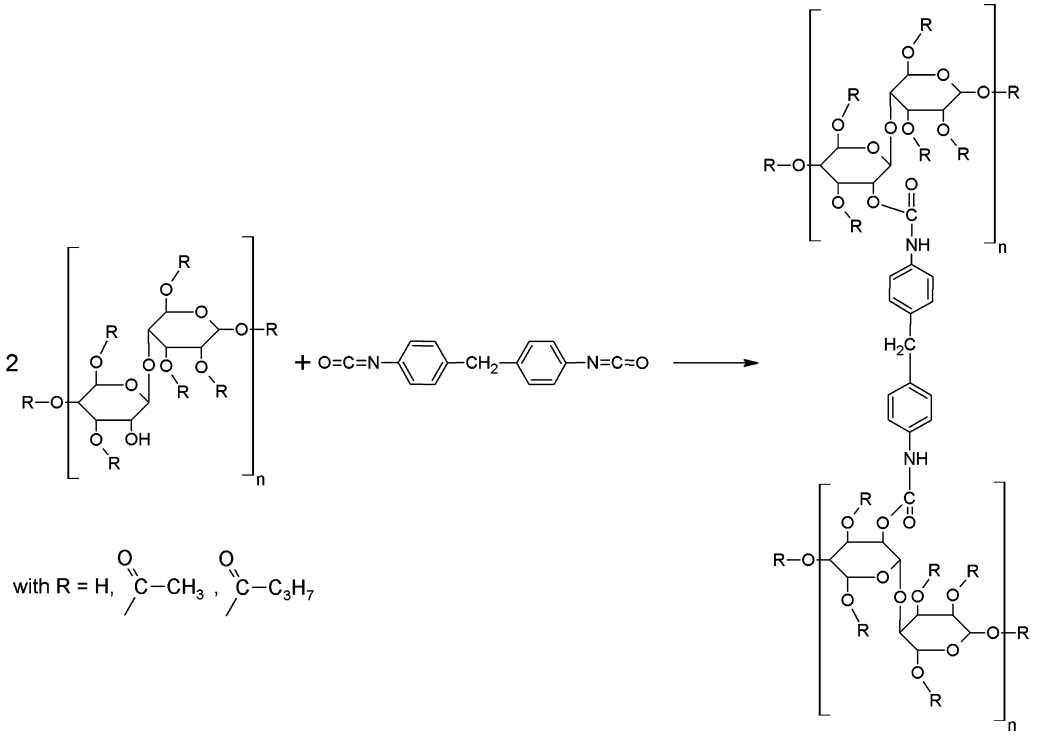

Scheme 2. Synthetic scheme for the preparation of a cross-linked CAB/MDI microcapsule.

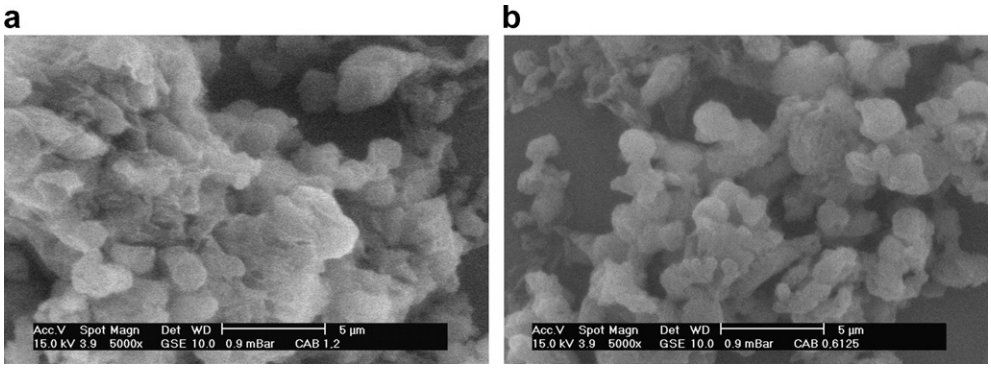

Fig. 1. Scanning electron micrographs of CAB/MDI microcapsules prepared with different amounts of CAB: 1.25%-wt (a) and 0.625%-wt (b).

is influenced by the rate of polycondensation, the modification of the nature of the components and the composition of this phase.

Furthermore, the morphology of the particles may be altered by theses parameters. The swellability of the polymer film allows the water diffusion in the organic phase and then promotes urea linkage since the polymeric film was formed and grown in the organic phase as described by Pensé, Vauthier, and Benoit (1994). The increase viscosity in the medium influences the formation of aggregated microcapsules. This mass coagulation is thought to be the result of a relatively vigorous stirring arrangement and insufficient stabilization of the initial CAB droplets. Sorbitan monooleate is apparently not a suitable stabilizer for this suspension when the polycondensation occurs.

The characterization of the chemical structure of the wall membrane is informative for the performance of the encapsulation experiments and for quantitative identification of the polymer formed during the process. The completion of polycondensation reaction between MDI and CAB was confirmed by FT-IR analysis. FT-IR spectra of MDI, CAB, DSP and microcapsules containing DSP are presented in Fig. 2. The following groups are relevant to the investigations reported here: OH (broad band at 3500 cm^{-1}); isocyanate (2280–2270 cm^{-1}); urea (1650 cm^{-1}) and urethane (1710 cm^{-1}). As seen in Fig. 2, the spectrum exhibits absorption bands at 1740–1700 cm^{-1} for the C═O stretching of urethane and at 1710–1650 cm^{-1} for urethane–urea formation. N—H stretching is evidenced with a broad band lying in the 3450–3300 cm^{-1} range. The C—H asymmetrical and symmetrical stretchings due to the methyl and methylene groups are observed between 2925 and 2854 cm^{-1}. The appearance of C—O—C stretching at 1130 cm^{-1}, and ═C—H bending at 880–750 cm^{-1} are also observed. The observed bands at 1262 and 1130 cm^{-1} can be assigned to —P═O groups of phosphate anion and the stretching mode of PO_4^{3-} at 954 cm^{-1} is also observed. FT-IR spectrum of microcapsules also contains characteristics bands of MDI at 1600, 1410 and 820 cm^{-1} assigned, respectively, to C═C stretching, C—C stretching and C—H bending in aromatic groups. Furthermore, the spectrum clearly shows that DSP was successfully microencapsulated, as it results from the presence of characteristic absorption bands at 1071, 984 and 866 cm^{-1} phosphate stretching vibrations.

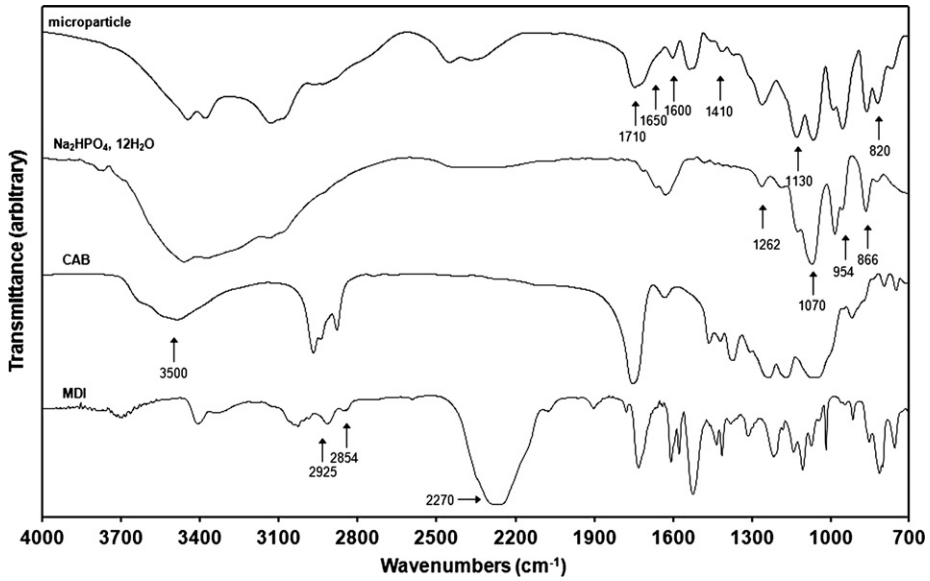

Fig. 2. FT-IR spectra of raw materials prior to encapsulation and the resulting microcapsules (batch 9).

Table 2
Preparation of microparticles

No. of batch	Continuous phase (%-wt)		Yield[a] (%)	Salt content[b] (%)	Glass temperature (°C)	State and surface, appearance of microparticles[e]
	CAB[c]	MDI[d]				
1	0.6125	2.5	18.7	79.2	123	Thin and smooth wall, few aggregated
2	1.25	2.5	54.1	75.5	123.5	Thin wall, fragment, aggregated
3	2.5	2.5	72.4	61.1	125	Well defined, smooth surface, less fragments
4	5	2.5	67.1	57.7	127.4	Rough surface, aggregated
5	10	2.5	50.4	40	128.2	Rough and irregular surface, fragments, very agglomerated
6	2.5	0	33.1	49	120.3	No capsules formed
7	2.5	0.5	63.6	58.5	128	Very brittle, thin and smooth wall
8	2.5	1	70.6	68.7	127.1	Brittle, porous, thin and regular surfaces, well defined
9	2.5	2	73.2	71.4	xxx	Less porous, few fragments, well defined
10	2.5	5	58.5	46.5	xxx	Rough and spongy surface, fragments, aggregated capsules
11	2.5	10	40.1	40.3	xxx	Fragments, rough surface, aggregated

Influence of CAB (and MDI) amount introduced on microparticle characteristics: yield, salt content, glass temperature and appearance of microcapsules.
[a] The yield is identical to monomer conversion.
[b] Determined by TGA.
[c] Solubilized in 30 ml chloroform.
[d] Solubilized in 30 ml toluene.
[e] Observed by SEM.

The cellulosic compound is cross-linked through the formation of urethane bonds. Thus, the membrane formation could be analyzed either by the lack of the vibration band of hydroxyl groups of the CAB and with the decrease (or disappearance) of the vibration band of isocyanate groups of MDI.

3.2. Influence of the amount of CAB on chemical structure

In this set of experiments, the particle size was kept constant while the amount of CAB has been modified, and the MDI amount is equal to 2.5%-wt. The formation of the porous membrane is controlled by the diffusion of the water through the dense layer. This diffusion is linked to the primary membrane permeability but also to the concentration in CAB that was increased in experiments from 1 to 5. As a result, it seems that the microcapsule wall became less porous and less brittle when the CAB concentration was increased (Table 2). The effect can be related to the polymer increased precipitation rate during the early stage of the formation of the microcapsule shell, corresponding to the formation of the primary membrane or CAB wall. Thus, the CAB concentration influences the precipitation rate, and since the water molecules are less available, the shell permeability decreases.

FT-IR spectroscopy provides a good method of monitoring the processes that occur during the microencapsulation: the absorption bands of all the functional groups involved can be distinguished and can be readily interpreted quantitatively. FT-IR spectra of synthesized microcapsules containing hydrated salt are presented in Figs. 3 and 4. The FT-IR spectrum also indicates the completion

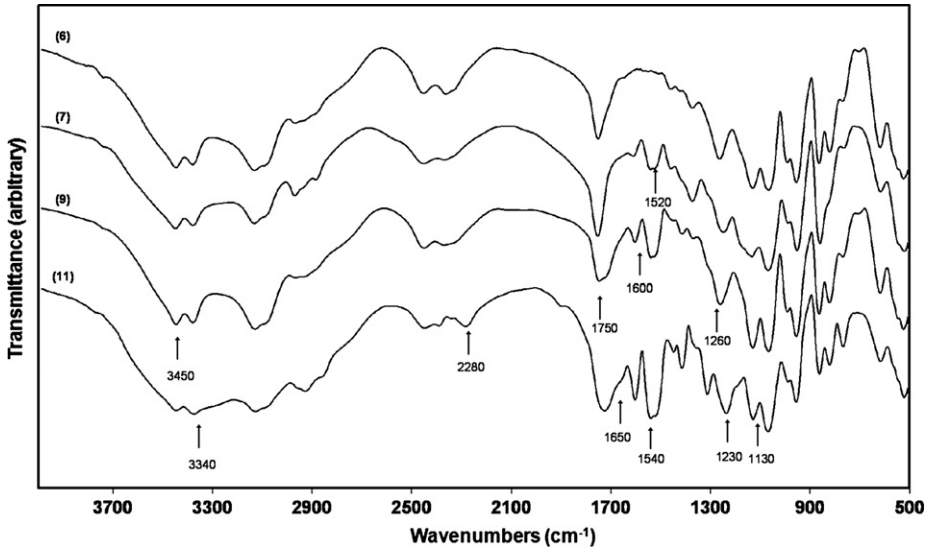

Fig. 3. FT-IR spectra of the microcapsules obtained by the reaction of CAB with various amounts of MDI: 0%-wt (batch 6), 0.5%-wt (batch 7), 2%-wt (batch 9) and 10%-wt (batch 11).

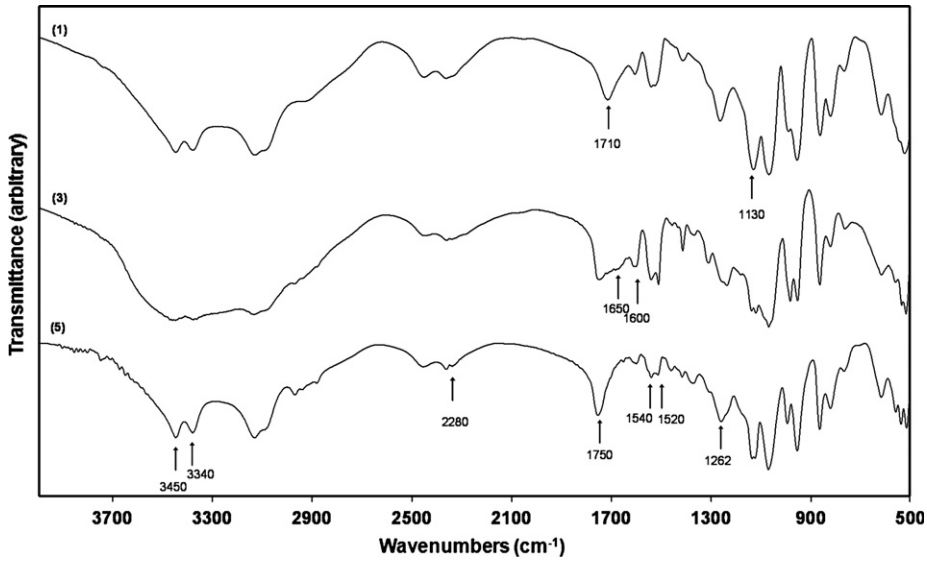

Fig. 4. FT-IR spectra of the microcapsules obtained by the reaction of MDI with various amounts of CAB: 0.6125%-wt (batch 1), 2.5%-wt (batch 3) and 10%-wt (batch 5).

of the reaction between isocyanate and cellulose by the disappearance of the NCO absorption band at 2280 cm^{-1} for amount of MDI above 5% and appearance of the N—H and C=O. Moreover, C=C stretching in the phenylene ring shows up at 1600 cm^{-1}.

All compounds show well defined, strong carbonyl absorption bands, in a fairly broad wavenumber range of 1600–1760 cm^{-1}. The results of the deconvoluted FT-IR spectra in the 1575–1800 cm^{-1} region are shown in Table 3. The region contains four main components at 1751, 1710, 1663 and 1605 cm^{-1}. The first one is usually assigned to the ester carbonyl groups of the CAB, the second one to urethane C=O stretching, the third one to urea and the last one to the aromatic C=C stretching.

The reaction of MDI with water at the oil–water interface forms urea linkage illustrated by the presence of urea band at 1663 cm^{-1}, which tends to decrease from 5%-wt of CAB. This result suggests a competitive mechanism between the formation of urea and urethane linkages. In order to check the previous hypothesis, the various experiments were analyzed by EDAX. These results are shown in Fig. 5 where the ratio O/(C + O) (in %) is expressed with varying CAB amount.

Table 3
Quantitative analysis of the carbonyl region (1800–1575 cm^{-1}) of FTIR spectra by peak deconvolution

No. of batch	ν(C=C) (%) 1605 cm^{-1}	ν(C=O) (%) urea 1663 cm^{-1}	ν(C=O) (%) urethane 1710 cm^{-1}	ν(C=O) (%) ester 1751 cm^{-1}
1	22.6	22.1	41.3	13.9
2	24.8	22.1	29.8	23.3
3	23.8	22.0	23.0	31.3
4	19.2	13.7	16.0	51.0
5	9.1	5.6	18.8	66.5
7	6.9	0.0	4.1	89.0
8	12.6	7.9	21.8	57.7
9	18.2	11.5	31.6	38.8
10	26.0	19.7	23.3	31.0
11	30.0	20.4	25.9	23.8

Fig. 6 shows the data from the EDAX and FT-IR experiments for batches no. 1–5. The data can be interpreted in terms of a variation of the O element in the medium. Thus, the data can be divided in two parts. First, the ratio decreases from experiment 1 to 4, suggesting that the MDI reacts with hydroxyl groups from the CAB and water molecules to form urethane and urea bonds. Nevertheless, as the accessibility of the OH functions decreases faster with the incorporation of CAB, the urethane fraction also decreases whereas the urea fraction remains constant. When the amount of CAB is weak, the formation of urea bond is governed by the possibility of the water molecules to diffuse through the primary membrane. Since the polymer was formed and grown in the organic phase, the modification of the components and composition of this phase should affect the course of the polycondensation reaction. Furthermore, the accessibility of the hydroxylic functions in the CAB molecules in accordance to their chemical structure can be correlated with their ability to induce polycondensation reaction and formation of urethane linkage. Secondly, an increase in CAB amount leads to a denser network characterized by a multilayer microcapsule. Thus, the water molecules diffusion becomes more difficult and promotes the decrease of the urea fraction.

We can observe that a too important amount of CAB leads to a ratio increase correlated with an increase in the part of urethane. All the CAB does not settle on the droplet surface and remains solubilized in the reactional medium to react thereafter with the MDI. These oligomers settle on the particle surface at the time of the stages in recovery of the microcapsules.

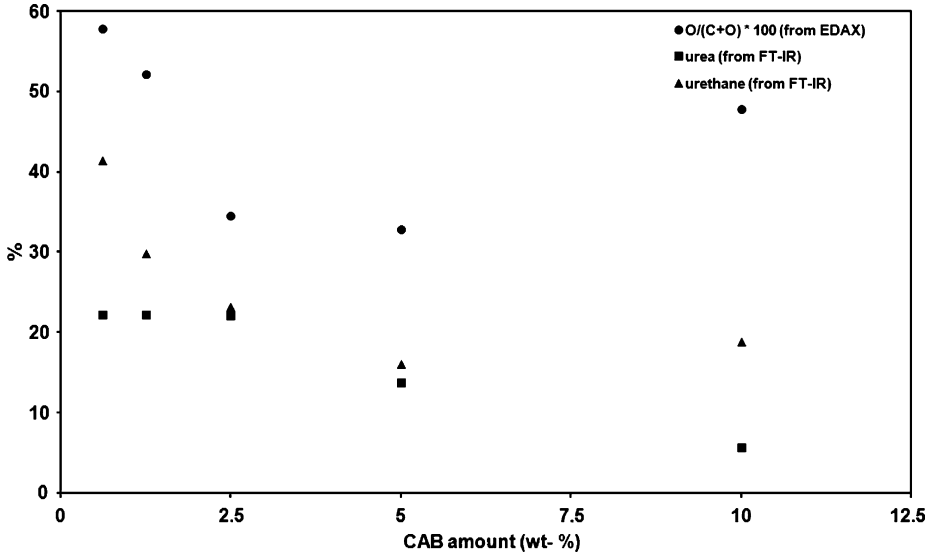

Fig. 5. Influence of the amount of CAB on the chemical structure of the microcapsules.

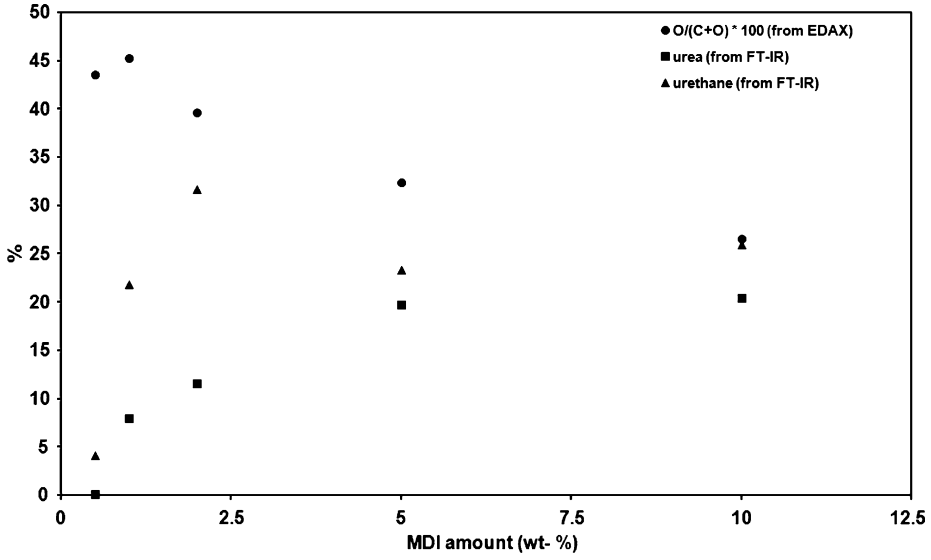

Fig. 6. Influence of the amount of MDI on the chemical structure of the microcapsules.

3.3. Influence of the amount of MDI, on chemical structure

In these experiments, the particle size was kept constant while changing the amount of MDI in these experiments, with 2.5%-wt of CAB.

Preliminary experiments realized with CAB demonstrated that it was necessary to introduce a minimum amount of cross-linking agent to get the formation of individual and sufficiently stable microcapsules. Among the tested cross-linking agents, MDI led to the best results between different isocyanate such as isophorone diisocyanate (IPDI), toluene diisocyanate (TDI) and MDI. In fact, polymers formed from them to synthesize the shells of microcapsules are less permeable. In previous work, Lukaszczyk and Urbas (1997) reported the same considerations and underlined the fact that higher amounts of isocyanate are required. In order to decrease the fragility of the wall, the concentrations in MDI were increased in batches 7–11 to promote urethane linkages (Table 2).

With an amount of 0.5%-wt of MDI and 2.5%-wt of CAB, only the urethane linkages appear whereas with the increase of MDI, the final structure presents the two bonds ($C{=}O_{ester}$ and $C{=}O_{urethane}$) (Fig. 3). The results of deconvolution (Table 3) show that a higher amount of MDI promotes the formation of urea. It suggests that when the accessibility of hydroxylic functions of CAB is not available, the MDI reacts with the water diffused through the wall. Thus, in the competitive mechanism the reaction with CAB is mainly favored.

The chemical structure of the membranes is strongly influenced by the increase of the amount of cross-linker as Fig. 6 shows it. Indeed, the ratio C/(C + O) presents a

maximum for a amount of MDI of 1%-wt then decreases during the increase of this amount to reach a value limit near 30%. This increasing is initially linked to the formation of urethane bonds which is strongly privileged for weak rate of MDI since OH are mainly accessible. In the second time, this formation of bond urethane is accompanied by the urea (and biuret) formation implying ratio decrease. The formation of biuret increases the proportion of carbon in the wall.

Whatever the rate of CAB and introduced MDI is, it appears that the formation of the urethane bonds is favorized. The formation of the urea bonds is only possible if the water molecules can diffuse through the network in CAB, meaning for weak introduced amounts. It is also noticed that the urea formation never exceeds 20%. The formation of the urethane bond is linked to the possibility of reaction between the hydroxyl function and the isocyanate. It increases up to an amount of 30% of MDI and then remains almost constant.

As a result of all combined effects, the organic phase composition can play a main role during the two steps of the polymeric shell formation. The first step consists in the formation of the primary membrane by the CAB precipitation. The amount introduced affects the permeability properties of the membrane and therefore influences the success of the second step, e.g. the cross-linking of the coating. The formation of a dense primary membrane can stop the growth of the shell, leading to very brittle microcapsules. This phenomenon could persist in the systems containing 0–1%-wt of MDI.

3.4. Glass transition temperature (T_g)

The permeability properties of the microcapsules are governed by the thermal properties of microcapsules wall membranes. Since the heating rate influences the transition around the T_g and the values presented in Table 2 are not absolute but useful for purposes of comparison. T_g changes recorded can be related to some physicochemical changes occurring in the polymer during solvent evaporation process (Torres et al., 1998) e.g. it is closely related to the film formation. The T_g of microcapsules without MDI is lower than the one of the raw CAB, 120.3 and 133 °C, respectively. Thus, the processing conditions and the presence of DSP drastically reduced the T_g, indicating a plasticizing effect of the core material, DSP. The cross-linking reaction between CAB and MDI causes a decrease in the T_g value. Vidal, Fichet, Laskar, and Teyssié (2006) have observed similar phenomenon and this evolution was related to a decrease in the extent of hydrogen bonding. Besides, the glass transition temperature of capsule wall was found to increase with increasing amounts of CAB and to depend on the amount of core material (Ichikawa, 1994). The increase of CAB amount results in CAB network with higher cross-link density since the $NCO/OH_{accessibles}$ molar ratio increases and consequently higher T_g value (Cunha, Melo, Veronese, & Forte, 2004).

3.5. Effect on encapsulation yield

The microencapsulation yield was dependent on a good emulsification step of the two phases. A high concentration of surfactant was used to decrease the interfacial tension and thereby to obtain a monodispersed emulsion. Without neglecting the importance of the choice of the surfactants and their concentration, the other main parameter to obtain a good emulsification and a narrow droplet size distribution is the viscosity of the dispersed and continuous phases (Freitas, Merkle, & Gander, 2004). Arnaud et al. (1996) found the yield as a function of the organic phase viscosity. Such increase in dispersion viscosity, typically caused by higher concentration of the wall material, may be desirable to restrict the migration of the salt from the solidifying microparticles to the continuous phase (Yan et al., 1994) and thus improve its entrapment. So, the influence of polymer concentration is attributed to its effect on the viscosity and the solidification rate of the polymer phase. First, the increase of polymer solution viscosity delays salt diffusion through the polymer membrane. Second, a highly concentrated polymer solution precipitates quickly since the cross-linker amount required is weaker. Therefore, once the polymer is solidified, the encapsulated salt does not easily escape from the shell and thus the encapsulation efficiency remains high.

The increase of the cellulose acetate butyrate and MDI amounts increase the viscosity of the organic phase and as observed in Table 2, decrease the yield from 2.5%-wt of CAB and 2%-wt of MDI. Furthermore, at low concentration in CAB or MDI, the low yields shown in Table 2 are probably due to the low coating efficiency with these compounds. At a CAB concentration range from 2.5%-wt to 10%-wt in solution, a substantial part of cross-linker is required. The optimal yield was obtained when the ratio (MDI to CAB) was found in the range of 0.4–1.

4. Conclusions

Coating of the particle of polymer-salt systems with CAB as wall material and MDI as cross-linker by utilizing interfacial promoted polyreaction results in the preparation of polyurethane–polyurea microcapsules. The influence of every component was discussed in terms of chemical structure in order to determine the optimal formulation. This latter is based on the formation of the urethane bond offering high encapsulation yield, salt content and optimal physical aspect of the microcapsules.

Thus, the mass of microcapsules recovered is optimal for amount of CAB and MDI in the range of 2.5–5%-wt. A compact structure is obtained when the reagents are introduced in these better (optimal) proportions.

As the recovered masses are similar to the preceding ones, the surplus of introduced reagents does not react any more at the interface. These observations are in agreement with the results obtained by EDAX.

References

Arnaud, P., Boue, C., & Chaumeil, J. C. (1996). Cellulose acetate butyrate microcapsules for controlled release of carbamazepine. *Journal of Microencapsulation, 13*(4), 407–417.

Arshady, R. (1989). Review preparation of microspheres and microcapsules by interfacial polycondensation techniques. *Journal of Microencapsulation, 6*(1), 13–28.

Arshady, R., & George, M. H. (1993). Suspension, dispersion, and interfacial polycondensation: A methodological survey. *Polymer Engineering and Science, 33*(14), 865–876.

Canbazoğlu, S., Şahinaslan, A., Ekmekyapar, A., Aksoy, Ý. G., & Akarsu, F. (2005). Enhancement of solar thermal energy storage performance using sodium thiosulfate pentahydrate of a conventional solar water-heating system. *Energy and Buildings, 37*(3), 235–242.

Cunha, F. O. V., Melo, D. H. R., Veronese, V. B., & Forte, M. M. C. (2004). Study of castor oil polyurethane-poly(methyl methacrylate) semi-interpenetrating polymer network (SIPN) reaction parameters using a 2^3 factorial experimental design. *Materials Research, 7*(4), 539–543.

El Bahri, Z., & Taverdet, J. L. (2006). Elaboration and characterisation of microcaparticles loaded by pesticide model. *Powder Technology, 172*(1), 30–40.

Erkan, G., & Sariisik, M. (2004). Microencapsulation in textiles. *Colourage, 51*, 61–64.

Freitas, S., Merkle, H. P., & Gander, B. (2004). Microencapsulation by solvent extraction/evaporation: Reviewing the state of the art of microsphere preparation process technology. *Journal of Controlled Release, 102*(2), 313–332.

Fundueanu, G., Constantin, M., Esposito, E., Cortesi, R., Nastruzzi, C., & Menegatti, E. (2005). Cellulose acetate butyrate microcapsules containing dextran ion-exchange resins as self-propelled drug release system. *Biomaterials, 26*(20), 4337–4347.

Ghule, A., Bhonghale, C., & Chang, H. (2003). Monitoring dehydration and condensation processes of $Na_2HPO_4{\cdot}12H_2O$ using thermo-Raman spectroscopy.. *Spectrochimica Acta Part A, 59*, 1529–1539.

Giunchedi, P., Conti, B., Maggi, L., & Conte, U. (1994). Cellulose acetate butyrate and polycaprolactone for ketoprofen spray-dried microsphere preparation. *Journal of Microencapsulation, 11*(4), 381–393.

Griffin, W. C. (1949). Classification of surface active agents by HLB. *Journal of the Society of Cosmetic Chemists, 1*, 372–375.

Hawlader, M. N. A., Uddin, M. S., & Khin, M. M. (2003). Microencapsulated PCM thermal-energy storage system. *Applied Energy, 74*(1), 195–208.

Hirano, S., & Saitoh, T. S. (2002). Growth rate of crystallization in disodium hydrogenphosphate dodecahydrate. *Journal of Thermophysics and Heat Transfer, 16*(1), 135–140.

Hirano, S., Saitoh, T. S., Oya, M., & Yamazaki, M. (2001). Temperature dependence of thermophysical properties of disodium hydrogenphosphate dodecahydrate. *Journal of Thermophysics and Heat Transfer, 15*(3), 340–346.

Hong, K., & Park, S. (1999). Preparation of polyurethane microcapsules with different soft segments and their characteristics. *Reactive & Functional Polymers, 42*, 193–200.

Ichikawa, K. (1994). Dynamic mechanical properties of polyurethane-urea microcapsules on coated paper. *Journal of Applied Polymer Science, 54*, 1321–1327.

Laskar, J., Vidal, F., Fichet, O., Gauthier, C., & Teyssié, D. (2004). Synthesis and characterization of interpenetrating networks from polycarbonate and cellulose acetate butyrate. *Polymer, 45*(15), 5047–5055.

Leitch, P., & Tassinari, T. H. (2000). New materials in the new millennium. *Journal of Industrial Textiles, 29*(3), 173–191.

Lukaszczyk, J., & Urbas, P. (1997). Influence of the parameters of encapsulation process and of the structure of diisocyanates on the release of codeine from resinate encapsulated in polyurea by interfacial water promoted polyreaction. *Reactive and Functional Polymers, 33*(2), 233–239.

Lyman, D. L. (1972). *Polyurethanes: The chemistry of the diisocyanate-diol reaction*. New York: Marcel Dekker.

Nelson, G. (1991). Microencapsulates in textile coloration and finishing. *Review of Progress in Coloration and Related Topics, 21*, 72–85.

Nelson, G. (2002). Application of microencapsulation in textiles. *International Journal of Pharmaceutics, 242*(1–2), 55–62.

Obeidat, W. M., & Price, J. C. (2005). Preparation and in vitro evaluation of propylthiouracil microspheres made of eudragit RL 100 and cellulose acetate butyrate polymers using the emulsion-solvent evaporation method. *Journal of Microencapsulation, 22*(3), 281–289.

Pause, B. (1995). Development of heat and cold insulating membrane structures with phase change material. *Journal of Coated Fabric, 25*(7), 59–68.

Pensé, A. M., Vauthier, C., & Benoit, J. P. (1994). Study of the interfacial polycondensation of isocyanate in the preparation of benzalkonium chloride loaded microcapsules. *Colloid and Polymer Science, 272*(2), 211–219.

Rege, M., Kovenklioglu, S., Yazici, R., Kalyon, D. M., Birinci, E., & Allred, A. (1999). Elastomeric coating of filler powders by slurry precipitation. *SPE ANTEC Technical Papers, 45*, 3489–3494.

Sandnes, B., & Rekstad, J. (2006). Supercooling salt hydrates: Stored enthalpy as a function of temperature. *Solar Energy, 80*, 616–625.

Torres, D., Boado, L., Blanco, D., & Vila-Jato, J. L. (1998). Comparison between aqueous and non-aqueous solvent evaporation methods for microencapsulation of drug-resin complexes. *International Journal of Pharmaceutics, 173*(1-2), 171–182.

Uda, K., & Hijikigawa, M. (1988). Moisture sensor containing cellulose acetate butyrate. *United States Patent*, US4773935.

Vidal, F., Fichet, O., Laskar, J., & Teyssié, D. (2006). Polysiloxan-cellulose acetate butyrate cellulose interpenetrating polymers networks close to true IPNs on a large range. Part II. *Polymer, 47*, 3747–3753.

Wang, Q., Fu, S., & Yu, T. (1994). Emulsion polymerization. *Progress in Polymer Science, 19*, 703–753.

Yadav, S. K., Suresh, A. K., & Khilar, K. C. (1990). Microencapsulation in polyurea shell by interfacial polycondensation. *AIChE Journal, 36*, 431–438.

Yan, C., Resau, J. H., Heweston, J., West, M., Rill, W. L., & Kende, M. (1994). Characterisation and morphological analysis of protein loaded poly(lactide-co-glycolide)microparticles prepared by water-in-oil-in-water emulsion technique. *Journal of Controlled Release, 32*(3), 231–241.

Yoshizawa, H., Kamio, E., Hirabayashi, N., Jacobson, J., & Kitamura, Y. (2004). Membrane formation mechanism of crosslinked polyurea microcapsules by phase separation method. *Journal of Microencapsulation, 21*(3), 241–249.

Zhang, X., Tao, X., Yick, K., & Wang, X. (2004). Structure and thermal stability of microencapsulated phase-change materials. *Colloid and Polymer Science, 282*(4), 330–336.